

ORIGINAL ARTICLE

# Angiotensin II receptor blocker irbesartan attenuates cardiac dysfunction induced by myocardial infarction in the presence of renal failure

Ryo Watanabe<sup>1</sup>, Jun-ichi Suzuki<sup>2</sup>, Kouji Wakayama<sup>2</sup>, Hidetoshi Kumagai<sup>2</sup>, Yuichi Ikeda<sup>3</sup>, Hiroshi Akazawa<sup>3</sup>, Issei Komuro<sup>3</sup> and Mitsuaki Isobe<sup>1</sup>

The activity of the renin–angiotensin system is known to be a key factor in the pathophysiology of heart failure and renal failure. Irbesartan, an angiotensin II receptor blocker, has non-hemodynamic cardiovascular and renal protective effects. However, the effect of irbesartan on heart failure complicated by renal failure has not yet been elucidated. Thus the purpose of this study was to evaluate the effect of irbesartan on the pathophysiology of cardiorenal syndrome in a rat model. Subtotal nephrectomy (NTX) was performed in rats using a two-step surgical procedure. Twenty-eight days after NTX, myocardial infarction (MI) was induced by ligation of the left anterior descending coronary artery. The animals were orally administered vehicle or irbesartan (10 mg kg<sup>-1</sup> day<sup>-1</sup>) after NTX. The hearts were harvested 28 days after MI. MI with NTX model rats showed an impaired post-MI survival rate and enhanced cardiac inflammation in comparison to MI without NTX rats. Although irbesartan treatment did not improve the survival rate, it suppressed cardiac inflammation, left ventricular function decline, cardiac fibrosis, hypertrophy of cardiomyocytes and renal fibrosis in MI with NTX rats. Moreover, increases in protein expression levels related to oxidative stress and inflammation (NADPH oxidase 4, phospho-nuclear factor- $\kappa$ B and phospho-c-Jun) observed in the hearts of non-treated MI with NTX rats were attenuated by irbesartan treatment. These effects of irbesartan treatment were independent of blood pressure. We conclude that irbesartan has a cardioprotective effect after MI when renal dysfunction is present.

*Hypertension Research* (2016) 39, 237–244; doi:10.1038/hr.2015.141; published online 10 December 2015

**Keywords:** angiotensin II receptor blocker; cardioprotective effect; cardiorenal syndrome

## INTRODUCTION

Cardiorenal syndrome is defined as the harmful interaction between the heart and kidneys. In fact, chronic kidney disease increases the risk of cardiovascular diseases.<sup>1–5</sup> Therefore, treatment to regulate the harmful interaction between the heart and kidneys is important. The activity of the renin–angiotensin system (RAS) is known to be a key factor in the development of heart failure and renal failure.<sup>6–10</sup> Myocardial infarction (MI) is a common antecedent event that predisposes a patient to congestive heart failure. Downstream oxidative stress and inflammatory responses of angiotensin II (Ang II) type 1 receptor (AT1R) signaling cause myocardial damage, such as cardiac hypertrophy and fibrosis.<sup>8,11–13</sup> This event is known as ventricular remodeling after MI, which leads to heart failure. Additionally, the activation of the RAS is one of the characteristics of renal failure. A previous study reported that renal injury deteriorates remodeling after MI through excessive RAS activation.<sup>14</sup> Ang II receptor blockers (ARBs) have been widely used as antihypertensive drugs. Irbesartan, an ARB, has non-hemodynamic cardiovascular and renal protective effects of the blockade of AT1R.<sup>15,16</sup> However, the effectiveness of

irbesartan on cardiac dysfunction complicated by renal dysfunction has not yet been established. Many chronic kidney disease patients are more likely to die of cardiovascular disease than end-stage renal disease and dialysis.<sup>17</sup> Furthermore, it has been reported that MI is more likely to develop in end-stage renal disease patients within 2 years after initiating dialysis therapy, and the mortality in these patients is high.<sup>4</sup> Thus we investigated whether irbesartan has a treatment effect on adverse myocardial remodeling after MI with renal failure. In this study, we demonstrate that irbesartan treatment may be promising as a new treatment approach to cardiorenal syndrome. Irbesartan offers significant potential to attenuate myocardial damage induced by ischemia when renal dysfunction is present.

## METHODS

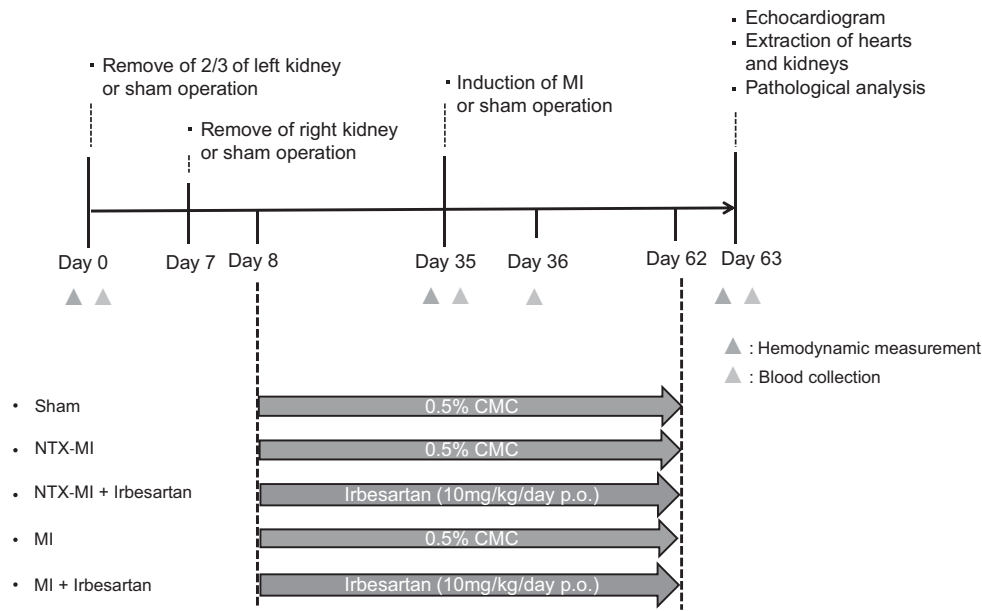
### Experimental protocols and animal model

Figure 1 shows the experimental protocol of this study.

Male Sprague-Dawley rats (6–8-weeks old; body weight approximately 200–250 g) were purchased from CLEA Japan (Tokyo, Japan). The rats were anesthetized with 50 mg kg<sup>-1</sup> of sodium pentobarbital i.p. immediately before

<sup>1</sup>Department of Cardiovascular Medicine, Tokyo Medical and Dental University, Tokyo, Japan; <sup>2</sup>Department of Advanced Clinical Science and Therapeutics, The University of Tokyo, Tokyo, Japan and <sup>3</sup>Department of Cardiovascular Medicine, The University of Tokyo, Tokyo, Japan  
Correspondence: Dr J-i Suzuki, Department of Advanced Clinical Science and Therapeutics, The University of Tokyo, 7-3-1 Hongo, Bunkyo, Tokyo 113-8655, Japan.  
E-mail: junichisuzuki-circ@umin.ac.jp

Received 18 April 2015; revised 30 October 2015; accepted 16 November 2015; published online 10 December 2015



**Figure 1** Experimental protocol. A full color version of this figure is available at the *Hypertension Research* journal online.

the operation. The rat model of 5/6 nephrectomy (NTX) was made using a two-step surgical procedure as described previously.<sup>18,19</sup> A Gemini Cautery Kit (Braintree Scientific, Braintree, MA, USA) was used to cauterize the left kidney (2/3 of the kidney mass) after laparotomy, and then the kidney stump was returned to the abdominal cavity on Day 0. A week later, the right kidney was removed by cutting the right renal vessels and ureter after it was ligated by a silk suture (Day 7). In total, 5/6 of the kidney mass was removed. Four weeks after NTX, MI was induced by ligation of the left anterior descending coronary artery as described previously<sup>20</sup> (Day 35). The hearts were harvested on Day 63. All animal experiments were approved by the Institutional Animal Care and Use Committee of Tokyo Medical and Dental University. These experiments were conducted according to the National Research Council's guidelines.

### Treatment

Irbesartan was provided by Shionogi (Japan). The drug was dissolved in 0.5% carboxymethylcellulose (CMC) solution immediately before use. The dose of irbesartan was selected according to previous studies reporting the pharmacological property and organ-protective effect of irbesartan.<sup>16,21,22</sup> The rats were assigned to five groups as follows: (i) Sham (oral administration of 0.5% CMC solution daily in sham operation), (ii) NTX-MI (oral administration of 0.5% CMC daily in the MI with 5/6 nephrectomy (NTX-MI) model), (iii) NTX-MI + irbesartan (oral administration of irbesartan (10 mg kg<sup>-1</sup>) daily in the NTX-MI model), (iv) MI (oral administration of 0.5% CMC daily in the MI model (sham NTX operation)), and (v) MI+irbesartan (oral administration of irbesartan (10 mg kg<sup>-1</sup>) daily in the MI model (sham NTX operation)). The detailed procedure is shown in Figure 1.

### Hemodynamic measurement

The blood pressure of all rats was evaluated on Days 0, 35 and 63. Hemodynamic measurement on Days 0 and 35 was performed before the operation. The blood pressure (systolic, diastolic and mean pressure) was measured in conscious rats using a tail-cuff system (BP-98A, Softron, Tokyo, Japan). Before the study was initiated, the rats were adapted to the apparatus for at least 5 days.

### Echocardiogram

Transthoracic echocardiography was performed on animals anesthetized by i.p. administration of pentobarbital sodium (25 mg kg<sup>-1</sup>) on Days 0, 35 and 63. An echocardiography machine with a 7.5-MHz transducer (Nemio, Toshiba, Tokyo, Japan) was used for left ventricular M-mode echocardiographic

recording. A 2D targeted M-mode echocardiogram was obtained along the short-axis view of the left ventricular (LV) papillary muscles.<sup>23</sup> The percentage of LV ejection fraction (LVEF), end-diastolic LV diameter (LVDd) and end-systolic LV diameter (LVDs) were calculated from the M-mode recordings.

### Blood examination

Blood samples were collected in heparinized microtubes and subjected to centrifugation on Days 0, 35, 36 and 63. The supernatant was stored at -80 °C until use. The creatinine (index of renal dysfunction) and cardiac troponin T (index of myocardial injury) levels in the serum were measured by SRL (Tokyo, Japan). Measurement of the serum creatinine level on Days 0 and 35 was performed before the operation.

### Histopathological examination

Hearts and kidneys were harvested immediately after all rats were killed by cutting of the abdominal aorta under anesthesia after an echocardiographic examination on Day 63. The hearts were divided into the apex-, midventricular- and basal-level slices. Formalin-fixed midventricular-level slices were used for histopathological examinations and immunohistochemistry. Formaldehyde-fixed paraffin-embedded sections from the midventricular-level heart slices of each group of rats were stained with the Mallory method and the silver impregnation method. The degree of cardiac hypertrophy in the non-infarct area after MI was estimated using silver impregnation staining.<sup>24</sup> We randomly selected 100 myocytes per sample section and measured the average cross-sectional size of the myocytes.<sup>12,25</sup> The myocardial infarct area (consisting of myocardial fibrosis) was estimated using Mallory staining. The stained area was defined as the infarcted area.<sup>12</sup> We measured the infarct thickness and infarct length in the Mallory-stained sections.<sup>26</sup> Histopathological analyses were performed using a computer-assisted analyzer (Scion Image Beta 4.0.2, Scion corporation, Frederick, MD, USA). Moreover, the content of collagen in the cardiac and renal tissue sections was measured using a Sirius Red/Fast Green Collagen Staining Kit (Chondrex, Redmond, WA, USA) according to the manufacturer's instruction. In this assay, collagen proteins were stained with Sirius Red, and non-collagenous proteins were stained with Fast Green. Subsequently, the dye was eluted from the tissue sections with dye extraction solution. The absorbance of the solution was measured at 540 and 605 nm, respectively, and the contents of collagen and non-collagenous proteins were determined. The content of collagen per tissue section was calculated as the ratio of collagen to total protein.<sup>27,28</sup>

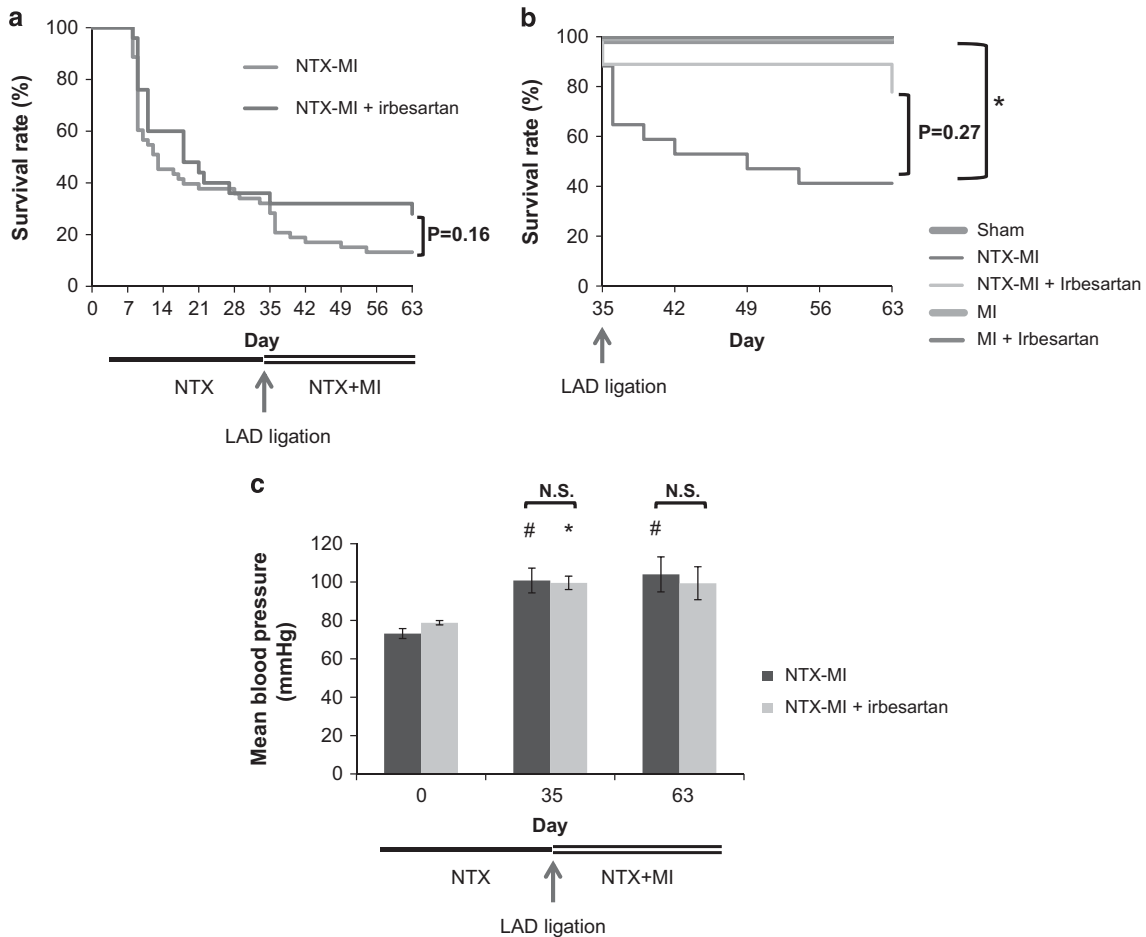


**Figure 2** Time course of the survival rate and blood pressure. (a) Survival curve from Day 0. (b) Post-MI survival curve. \* $P < 0.05$  vs. MI. (c) Time course of the mean blood pressure. NTX-MI,  $n = 6$ ; NTX-MI+irbesartan,  $n = 5$ . # $P < 0.05$  vs. NTX-MI on Day 0; \* $P < 0.05$  vs. NTX-MI+irbesartan on Day 0. NS, not significant. A full color version of this figure is available at the *Hypertension Research* journal online.

### Immunohistochemistry

Immunohistochemistry was performed to examine the degree of macrophage infiltration in the hearts on Day 63. Paraffin sections were incubated with primary antibodies against CD68 (as a marker of macrophages) (ED1, AbD Serotec, Oxford, UK) for 8 h at 4°C, washed in phosphate-buffered saline, followed by biotinylated secondary antibodies (Nichirei, Tokyo, Japan) at 5 mg ml<sup>-1</sup> for 30 min at room temperature. Finally, each section was reacted with AEC (aminoethyl carbazole complex) solution (Nichirei) for 5–30 min. We counted the number of CD68-positive cells in three randomly selected fields (original magnification, ×100) from the border zone between the infarct and non-infarct areas per sample section and used the average count.

### Extraction of proteins

To extract cardiac protein, frozen peri-infarct zone tissues from apex-level heart slices harvested on Day 63 were homogenized in lysis buffer (50 mM Tris-HCl (pH 7.5), 150 mM NaCl, 1% Triton X-100, 1% sodium deoxycholate, 1% sodium dodecyl sulfate (SDS)) containing a protease inhibitor cocktail tablet (Roche Diagnostic, Basel, Switzerland) and a phosphatase inhibitor tablet (Roche Diagnostic). The lysate was centrifuged at 14 000 g for 15 min. Protein concentrations of the supernatant were measured by a BCA protein assay (Bio-Rad, Milan, Italy) to equalize the protein concentrations of all samples. These protein samples were stored at -80°C and subsequently used as the samples for a western blotting analysis.

### Western blotting

Protein samples were mixed with an equal volume of 2×SDS sample buffer (0.5 M Tris-HCl (pH 6.8), 20% glycerol, 4% SDS, 0.05% bromophenol blue)

and incubated for 5 min at 95°C. The samples were separated by SDS-polyacrylamide gel electrophoresis with 10% acrylamide gel at 150 V and then transferred to a nitrocellulose membrane. The membranes were incubated overnight at 4°C with four primary antibodies: NADPH oxidase 4 (NOX4), phospho-c-Jun, phospho-nuclear factor-κB p65 subunit (NF-κB p65), and glyceraldehyde 3-phosphate dehydrogenase (GAPDH) (all from Cell Signaling Technology, Danvers, MA, USA). Later, the membranes were incubated with a secondary antibody (Amersham Biosciences, Piscataway, NJ, USA) for 1 h and developed using an ECL reagent (Thermo Fisher Scientific, Waltham, MA, USA). Enhanced chemiluminescence was detected with the LAS-1000 system (Fujifilm, Tokyo, Japan). The protein expression level was normalized to the GAPDH expression level and calculated as a fold change to the Sham group. This analysis was performed using the ImageJ software program (National Institutes of Health (NIH), Bethesda, MD, USA).

### Statistical analysis

All data are expressed as the mean ± s.e.m. Statistical analyses were performed using the Stat View software program (SAS Institute, Cary, NC, USA). Student's *t*-test was used to compare data between two groups. A comparison between three groups was conducted using analysis of variance followed by Fisher's Least Significant Difference test. The Tukey-Kramer method was performed to compare more than four groups. A survival analysis was performed using the Kaplan-Meier method with log-rank test. In the statistical analysis of the post-MI survival rate among multiple groups (Figure 2c), the *P*-value was corrected by Bonferroni's correction as follows:  $P\text{-value} \times 3$  tests of NTX-MI vs. MI,

**Table 1** The number of surviving animals and the survival rate at each time point

	Number of surviving animals			Survival rate from Day 0 (Figure 2a) (%)	Post-MI survival rate (Figure 2b) (%)
	Day 0	Day 35	Day 63		
Sham	4	4	4	100	100
NTX-MI	53	17	7	13.2	41.2
NTX-MI+irbesartan	25	9	7	28	77.8
MI	9	9	9	100	100
MI+irbesartan	9	9	9	100	100

Abbreviations: MI, myocardial infarction; NTX, nephrectomy.

NTX-MI vs. NTX-MI +irbesartan, and MI vs. MI+irbesartan. Differences were considered to be statistically significant at a value of  $P < 0.05$ .

## RESULTS

### Time course of the survival rate and blood pressure

Many rats died after the NTX procedure. The number of surviving animals and the survival rate at each time point are shown in Table 1. Irbesartan administration did not significantly improve the survival rates compared with vehicle administration (Figure 2a, NTX-MI = 13.2% vs. NTX-MI+irbesartan = 28%,  $P = 0.16$ ). We next determined the post-MI survival curve, which started on the onset of MI (Day 35) including the MI and MI+irbesartan groups, to demonstrate the effect of NTX on the prognosis after MI (Figure 2b). In the post-MI survival curve, the post-MI survival rate of the MI and MI+irbesartan groups were both 100%. Conversely, the post-MI survival rate of the NTX-MI group was 41.2%. This value was significantly lower than the MI group (Figure 2b, MI = 100% vs. NTX-MI = 41.2%,  $P < 0.05$ ). Although the post-MI survival rate of the NTX-MI+irbesartan group was 77.8%, there was no significant difference in the post-MI survival rate between the NTX-MI and NTX-MI+irbesartan groups (Figure 2b, NTX-MI = 41.2% vs. NTX-MI+irbesartan = 77.8%,  $P = 0.27$ ). The mean blood pressure was constantly elevated after NTX (on or after Day 35) compared with the sample taken before NTX on Day 0 ( $P < 0.05$ , Figure 2c). On the other hand, MI operation had no effect on the blood pressure compared with the sample taken before MI on Day 35 (Figure 2c). Additionally, irbesartan treatment had no effect on the blood pressure (Figure 2c).

### Effect of irbesartan treatment on cardiac damage and dysfunction

A previous study reported that the serum troponin T level, reflecting the extent of cardiac damage in a rat MI model, was rapidly elevated within 24 h after MI.<sup>26</sup> Therefore, we compared the serum troponin T levels on the day after MI operation (Day 36). Although the serum troponin T levels increased in the NTX-MI group compared with the Sham group ( $P < 0.05$ ), there was no significant difference between the NTX-MI and NTX-MI+irbesartan groups (Figure 3a). Furthermore, we measured the collagen level in heart slices from each group to examine the severity of cardiac fibrosis. Although hearts from the NTX-MI group had elevated collagen levels compared with those of the Sham group ( $P < 0.05$ ), the NTX-MI+irbesartan group showed that the increase of the cardiac collagen level was suppressed ( $P < 0.05$ , Figure 3b). The cardiac function was measured by echocardiography on Day 63. An M-mode echocardiogram after MI showed LVEF decline that was characterized by impaired anterolateral (infarct area) wall motion in the NTX-MI group (Figures 3c and d). Although irbesartan treatment did not affect the anterolateral wall motion, as shown by the elevation of the LVEF value, the regional wall motion of the non-infarct area was improved in the NTX-MI+irbesartan group

compared with that of the NTX-MI group ( $P < 0.05$ , Figures 3c and d). Moreover, LV cavity expansion (LVDd and LVDs) was observed in the NTX-MI group compared with the Sham group ( $P < 0.05$ , Figures 3e and f). Although the difference in LVDd was not significant, ischemia-induced expansion of LVDs was significantly suppressed in the NTX-MI+irbesartan group compared with the NTX-MI group ( $P < 0.05$ , Figures 3e and f). Similarly, LVEF decline and LV cavity expansion were significantly suppressed in the MI+irbesartan group compared with the MI group ( $P < 0.05$ , Figures 3d–f). There were no significant differences in these echocardiographic parameters between the NTX-MI and MI groups (Figures 3d–f).

### Effect of irbesartan treatment on post-MI remodeling and remodeling-associated signaling in the heart

Left anterior descending ligation induced morphological changes associated with post-MI remodeling in the myocardium. We analyzed the infarct size, compensatory hypertrophy of the non-infarct area and cardiac inflammation to examine the effect of irbesartan treatment on the progression of post-MI remodeling. Mallory staining showed that the anterior wall (infarct area) was completely fibrotic in the NTX-MI and NTX-MI+irbesartan groups (Figure 4a), whereas it was virtually absent in the Sham group (data not shown). There was no significant difference regarding the infarct length and infarct thickness among all groups (Figures 4b and c). The NTX-MI and MI groups each showed an increase in the cardiomyocyte cross-sectional size compared with the Sham group ( $P < 0.05$ , Figures 4d and e). However, there was no significant difference in the cardiomyocyte cross-sectional size between the NTX-MI and MI groups (Figures 4d and e). Irbesartan treatment in both the NTX-MI and MI models suppressed the increase in cardiomyocyte cross-sectional size induced by ischemia ( $P < 0.05$ , Figures 4d and e). Severe macrophage infiltration was observed in the border zone between the infarct and non-infarct areas of the heart from the NTX-MI group, whereas it was absent in the Sham group (Figure 4f). Moreover, the number of infiltrating macrophages was significantly increased in the NTX-MI group compared with the MI group ( $P < 0.05$ , Figures 4f and g). This increased macrophage infiltration was significantly attenuated in the NTX-MI+irbesartan group ( $P < 0.05$ , Figures 4f and g). On the other hand, the MI and MI+irbesartan groups showed less macrophage infiltration. There was no significant difference in macrophage infiltration between the MI and MI+irbesartan groups (Figures 4f and g). Ang II signaling via AT1R activates the factors associated with oxidative stress and inflammation.<sup>29,30</sup> Therefore, we measured the protein expression of NOX4, c-Jun (the component of activator protein-1 (AP-1)) and NF- $\kappa$ B p65 to examine the mechanisms of the treatment effect of irbesartan. The expression levels of phospho-c-Jun and phospho-NF- $\kappa$ B p65 were used as indices of AP-1 and NF- $\kappa$ B activation, respectively. The expression of NOX-4, phospho-NF- $\kappa$ B p65 and

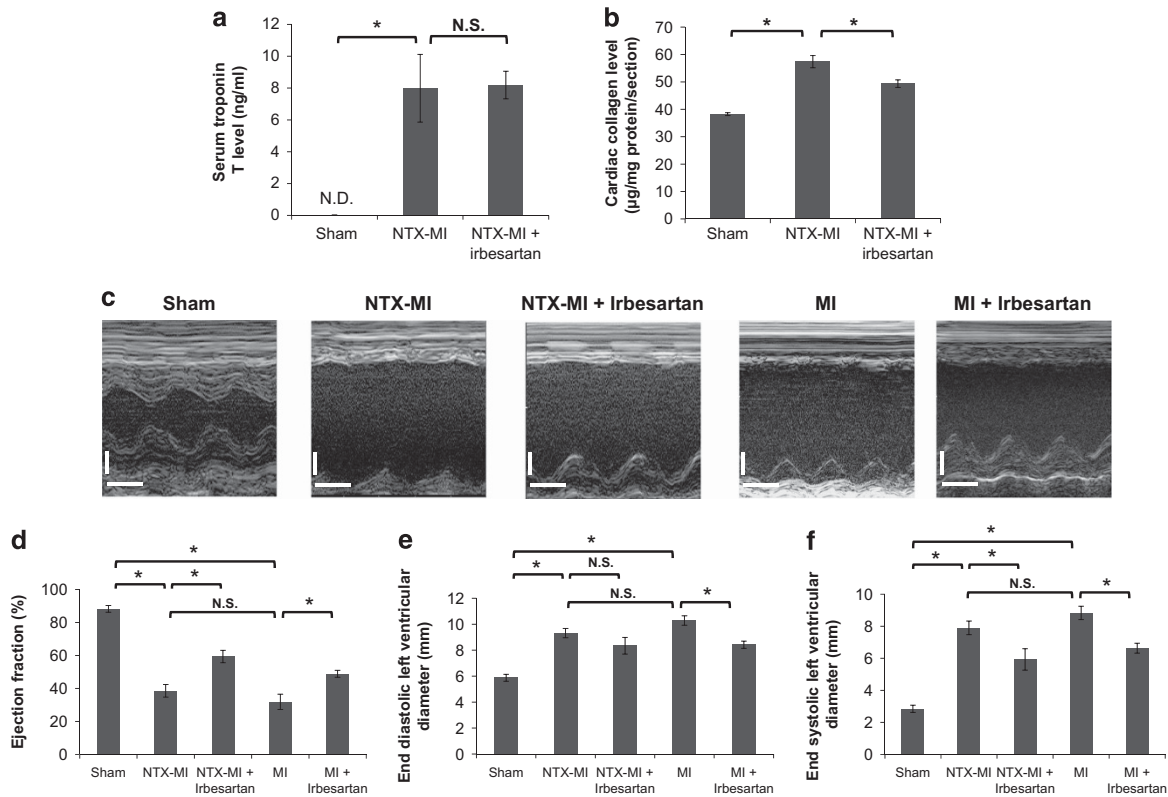


**Figure 3** Effect of irbesartan treatment on cardiac damage and dysfunction. (a) Serum troponin T level on Day 36. Sham,  $n=3$ ; NTX-MI,  $n=7$ ; NTX-MI + irbesartan,  $n=5$ . \* $P<0.05$ . ND, not detected. (b) Cardiac collagen level on Day 63. Sham,  $n=3$ ; NTX-MI,  $n=4$ ; NTX-MI+irbesartan,  $n=6$ . \* $P<0.05$ . (c) Representative M-mode echocardiograms on Day 63. Scale bars: 2 mm (vertical), 0.1 second (horizontal). A quantitative analysis of (d) the left ventricular ejection fraction (LVEF), (e) end-diastolic left ventricular diameter (LVDd) and (f) end-systolic left ventricular diameter (LVDs). Sham,  $n=4$ ; NTX-MI,  $n=7$ ; NTX-MI+irbesartan,  $n=7$ ; MI,  $n=9$ ; MI+irbesartan,  $n=9$ . \* $P<0.05$ .

phospho-c-Jun were significantly increased in the hearts from the NTX-MI group compared with the Sham group ( $P<0.05$ , Figures 4h and k). The increased expression of these factors was significantly suppressed in the NTX-MI+irbesartan group ( $P<0.05$ , Figures 4h and k).

#### Effect of irbesartan treatment on renal dysfunction

We measured the serum creatinine and renal collagen levels as markers of renal damage to examine the effect of irbesartan treatment on renal dysfunction in cardiorenal syndrome. The serum creatinine levels increased after NTX (on or after Day 35) compared with the sample taken before NTX on Day 0 ( $P<0.05$ , Figure 5a). On the other hand, MI operation did not affect the serum creatinine level on Day 63 compared with the sample taken before MI on Day 35 (Figure 5a). Irbesartan administration did not alter the level of serum creatinine (Figure 5a). The renal collagen level was significantly increased in the NTX-MI group compared with the Sham group on Day 63 ( $P<0.05$ , Figure 5b). This increase in the renal collagen level was significantly suppressed in the NTX-MI+irbesartan group ( $P<0.05$ , Figure 5b).

#### DISCUSSION

Cardiac disease is the main cause of death in chronic kidney disease patients.<sup>4</sup> A growing body of evidence suggests that renal injury enhances cardiac function decline and fibrosis after MI.<sup>31,32</sup> Our previous study revealed that excessive circulating RAS activation induced by renal dysfunction promotes oxidative stress and inflammation in the heart. This causes further deterioration of ventricular

dysfunction after MI.<sup>14</sup> In a model of combined renal and cardiac dysfunction, further activation of the RAS is present. Some ARBs are known to protect both the heart and kidney.<sup>33,34</sup> However, although ARBs can decrease the mortality and morbidity in patients with cardiovascular or renal dysfunction, they are not always prescribed to patients with combined cardiac and renal dysfunction in the clinical setting. Therefore, it is of the utmost importance to examine the effects of ARBs in combined cardiac and renal dysfunction. Irbesartan has a potent and highly selective AT1R-blocking effect with an elimination half-life from 11 to 15 h.<sup>35</sup> The long-lasting effect of irbesartan has been confirmed by its strong binding to AT1R and slow dissociating from AT1R compared with other ARBs, such as losartan and olmesartan.<sup>22,36</sup> Irbesartan demonstrates a renoprotective effect that is partly independent of its blood pressure-lowering effect in both the early and later stages of diabetic nephropathy.<sup>37,38</sup> Moreover, irbesartan has superior cardioprotective and renoprotective effects compared with losartan.<sup>39</sup> However, its cardioprotective effects in MI combined with renal failure have not been established. The present study shows that irbesartan administration could prevent cardiac damage when renal dysfunction and heart failure merge. We included the MI and MI+irbesartan groups (both sham NTX) to demonstrate the effect of NTX on the prognosis after MI. There was no significant difference in the echocardiographic parameters between the NTX-MI and MI groups in surviving animals. However, the post-MI survival rate of the NTX-MI group was 41.2%, whereas the post-MI survival rate of the MI and MI+irbesartan groups were both 100%. This result suggests that NTX aggravated the cardiac damage by MI and/or

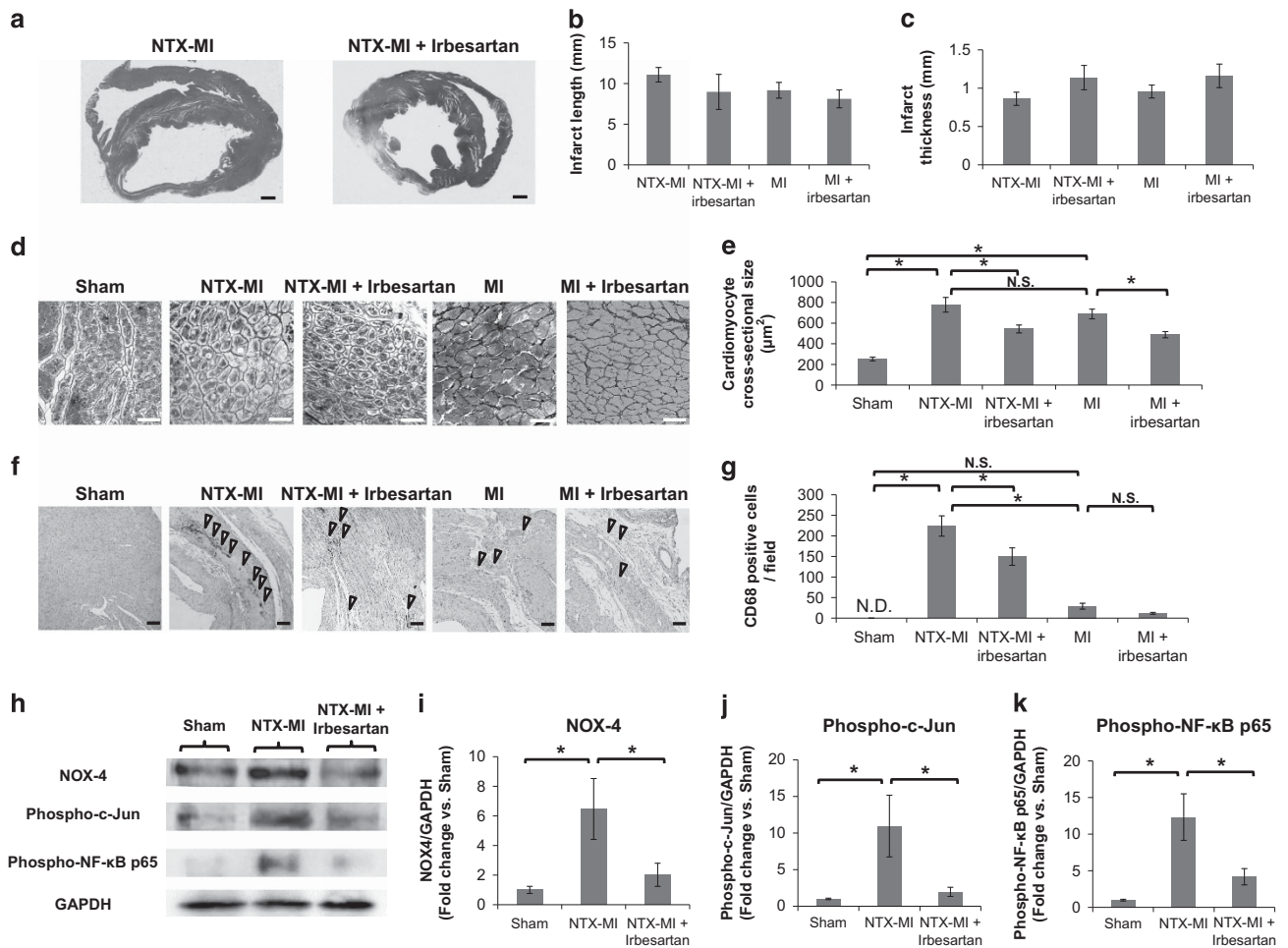


**Figure 4** Effect of irbesartan treatment on post-MI remodeling and remodeling-associated signaling in the heart. (a) Representative photomicrographs of Mallory-stained cross-sections from the NTX-MI and NTX-MI+irbesartan groups (magnification  $\times 10$ ; scale bars: 1 mm) on Day 63. Quantitative data of the (b) infarct length and (c) thickness. NTX-MI,  $n=6$ ; NTX-MI+irbesartan,  $n=6$ ; MI,  $n=7$ ; MI+irbesartan,  $n=7$ . (d) A representative photomicrograph of silver impregnation staining of the non-infarct area (magnification  $\times 400$ ; scale bars: 50  $\mu\text{m}$ ) and (e) quantitative comparison of the cardiomyocyte cross-sectional size in each group on Day 63. Sham,  $n=4$ ; NTX-MI,  $n=7$ ; NTX-MI+irbesartan,  $n=7$ ; MI,  $n=9$ ; MI+irbesartan,  $n=9$ . \* $P<0.05$ . (f) A representative photomicrograph of CD68 immunostaining (magnification  $\times 100$ ; scale bars: 100  $\mu\text{m}$ ) and (g) the number of infiltrating macrophages (CD68-positive cells) in the border zone between the infarct area and non-infarct area on Day 63. Sham,  $n=4$ ; NTX-MI,  $n=7$ ; NTX-MI+irbesartan,  $n=7$ ; MI,  $n=9$ ; MI+irbesartan,  $n=9$ . \* $P<0.05$ . (h) Representative western blottings of NADPH oxidase 4 (NOX4), phospho-c-Jun, phospho-nuclear factor- $\kappa\text{B}$  p65 subunit (NF- $\kappa\text{B}$  p65) and glyceraldehyde 3-phosphate dehydrogenase (GAPDH) in the peri-infarct tissues on Day 63. The relative expression of (i) NOX4, (j) phospho-c-Jun and (k) phospho-NF- $\kappa\text{B}$  p65. Sham,  $n=4$ ; NTX-MI,  $n=5$ ; NTX-MI+irbesartan,  $n=5$ . \* $P<0.05$ . A full color version of this figure is available at the *Hypertension Research* journal online.

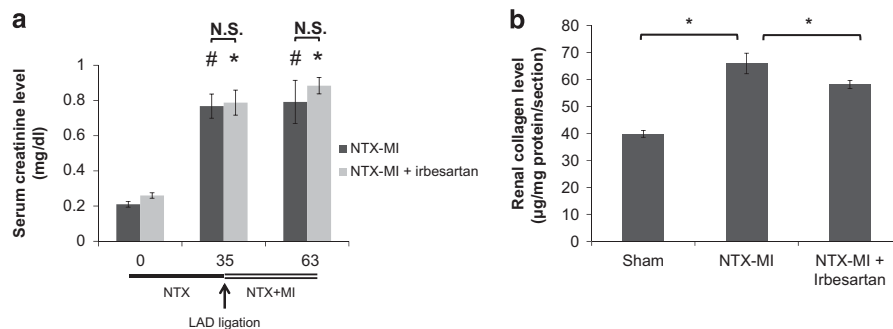


**Figure 5** Effect of irbesartan treatment on renal dysfunction. (a) Time course of the serum creatinine level. NTX-MI,  $n=6$ ; NTX-MI+irbesartan,  $n=5$ . # $P<0.05$  vs. NTX-MI on Day 0; \* $P<0.05$  vs. NTX-MI+irbesartan on Day 0. (b) Renal collagen level on Day 63. Sham,  $n=3$ ; NTX-MI,  $n=5$ ; NTX-MI+irbesartan,  $n=6$ . \* $P<0.05$ .

MI aggravated the renal damage. Hence, the high death rate of the NTX-MI group may be due to the progression of heart failure and/or renal dysfunction in the acute phase of post-MI remodeling. Similarly, in the post-MI survival rate, cardiac inflammation shown by macrophage infiltration was significantly enhanced in the NTX-MI group compared with the MI group. In contrast, the degree of cardiac inflammation shown by macrophage infiltration was relatively mild in the MI and MI+irbesartan groups. We speculate that these results in the MI and MI+irbesartan groups are attributed to the time course of post-MI remodeling.<sup>40–42</sup> On the other hand, irbesartan treatment did not significantly improve the post-NTX and -MI survival rates. However, enhanced inflammation in the NTX-MI model was significantly attenuated by irbesartan treatment. Inflammation is a critical response that induces cardiac remodeling in the acute phase after MI.<sup>43,44</sup> Additionally, this study revealed that irbesartan treatment suppressed the activation of oxidative stress-, inflammation- and cardiac remodeling-related proteins (NOX4, NF- $\kappa$ B and c-Jun of the AP-1 component) in the heart. Ang II induces the activation of NF- $\kappa$ B and AP-1 via AT1R and NOX4.<sup>29</sup> These Ang II-induced responses become the factor for inflammation and fibrosis in the end-organ damage.<sup>29,45–48</sup> Moreover, the enhancement of oxidative stress and inflammation, including the activation of NOXs and NF- $\kappa$ B, is induced by RAS activation in cardiorenal syndrome.<sup>14,46</sup> Enhanced inflammation mediates the harmful interaction between the heart and the kidney.<sup>4,49,50</sup> Therefore, we speculate that the antifibrotic and anti-inflammatory effects of irbesartan result from the inhibition of the activation of NF- $\kappa$ B, AP-1 and NOX4. Although the treatment effect of irbesartan did not improve the survival rate, our results suggest the possibility that the anti-inflammatory effect of irbesartan in the early phase of post-MI remodeling improves the prognosis after MI in the presence of renal dysfunction. Meanwhile, there was no difference in the serum troponin T levels between the NTX-MI and NTX-MI+irbesartan groups. Troponin T is an indicator of myocardium damage. The troponin T levels in a rat MI model peak within 24 h after ischemia.<sup>26</sup> This result suggests that the degree of cardiac damage by ischemia was comparable. Nevertheless, cardiac function decline after MI was significantly attenuated with irbesartan treatment in the surviving NTX-MI model animals. Moreover, irbesartan treatment suppressed macrophage infiltration, collagen deposition and cardiomyocyte hypertrophy during post-MI remodeling in the NTX-MI model. Fibrosis progresses to the non-infarct area from the infarct area in the heart, and compensatory hypertrophy is induced in the non-infarct area. The NTX-MI+irbesartan group showed less collagen deposition and a smaller cardiomyocyte cross-sectional size, although there was no difference in the infarct size compared with the NTX-MI group. These results suggest that irbesartan treatment prevented the progression of cardiac remodeling and improved the pathophysiology after MI in the presence of renal dysfunction. As expected, NTX promoted systemic arterial hypertension. In this study, irbesartan treatment showed cardioprotective effects without lowering the blood pressure. Hypertension is a major problem during ARB treatment. This result may demonstrate the clinical usefulness of irbesartan. Irbesartan treatment did not decrease the serum creatinine level elevated by NTX. An increase in the serum creatinine was shown as a side effect of RAS inhibition, including ARB treatment, in previous reports.<sup>3,51</sup> However, it was reported that an increase in the serum creatinine level was associated with improvement of long-term kidney function in ARB-treated patients.<sup>3</sup> Our data revealed that irbesartan treatment increased the serum creatinine level by approximately 11%, although this increase was not significant. Therefore, the serum creatinine level alone may be insufficient as a measure of the effect of irbesartan on

renal function. Similarly, we measured the renal collagen level to examine the effect of irbesartan treatment on renal dysfunction in cardiorenal syndrome. The renal collagen level reflects the degree of renal fibrosis.<sup>52</sup> An increase in the renal collagen level in the NTX-MI model was significantly suppressed by irbesartan treatment. These results suggest that irbesartan has a partial treatment effect on renal dysfunction. Although a sufficient treatment effect in the kidney was not observed, our data showed that low-dose irbesartan, which did not affect the blood pressure, suppressed cardiac remodeling after MI in the presence of renal dysfunction. We conclude that irbesartan treatment may be beneficial as a new approach for treating cardiorenal syndrome because heart failure is the main cause of death in patients with renal failure.

## CONFLICT OF INTEREST

The authors declare no conflict of interest.

## ACKNOWLEDGEMENTS

We thank Ms Noriko Tamura and Ms Yasuko Matsuda for excellent technical assistance. This study was supported by the Japan Society for the Promotion of Science (JSPS) KAKENHI Grant Number 25461122.

- 1 Go AS, Chertow GM, Fan D, McCulloch CE, Hsu CY. Chronic kidney disease and the risks of death, cardiovascular events, and hospitalization. *N Engl J Med* 2004; **351**: 1296–1305.
- 2 Bock JS, Gottlieb SS. Cardiorenal syndrome: new perspectives. *Circulation* 2010; **121**: 2592–2600.
- 3 House AA, Haapio M, Lassus J, Bellomo R, Ronco C. Therapeutic strategies for heart failure in cardiorenal syndromes. *Am J Kidney Dis* 2010; **56**: 759–773.
- 4 Bongartz LG, Cramer MJ, Doevendans PA, Joles JA, Braam B. The severe cardiorenal syndrome: 'Guyton revisited'. *Eur Heart J* 2005; **26**: 11–17.
- 5 Dickhout JG, Carlisle RE, Austin RC. Interrelationship between cardiac hypertrophy, heart failure, and chronic kidney disease: endoplasmic reticulum stress as a mediator of pathogenesis. *Circ Res* 2011; **108**: 629–642.
- 6 Siragy HM, Carey RM. Role of the intrarenal renin-angiotensin-aldosterone system in chronic kidney disease. *Am J Nephrol* 2010; **31**: 541–550.
- 7 Sun Y. Intracardiac renin-angiotensin system and myocardial repair/remodeling following infarction. *J Mol Cell Cardiol* 2010; **48**: 483–489.
- 8 Kim S, Iwao H. Molecular and cellular mechanisms of angiotensin II-mediated cardiovascular and renal diseases. *Pharmacol Rev* 2000; **52**: 11–34.
- 9 Zhang Y, Shao L, Ma A, Guan G, Wang J, Wang Y, Tian G. Telmisartan delays myocardial fibrosis in rats with hypertensive left ventricular hypertrophy by TGF- $\beta$ 1/Smad signal pathway. *Hypertens Res* 2014; **37**: 43–49.
- 10 Zouein FA, Zgheib C, Hamza S, Fuseler JW, Hall JE, Soljancic A, Lopez-Ruiz A, Kurdi M, Booz GW. Role of stat3 in angiotensin II-induced hypertension and cardiac remodeling revealed by mice lacking stat3 serine 727 phosphorylation. *Hypertens Res* 2013; **36**: 496–503.
- 11 Sun Y. Myocardial repair/remodelling following infarction: roles of local factors. *Cardiovasc Res* 2009; **81**: 482–490.
- 12 Maejima Y, Okada H, Haraguchi G, Onai Y, Kosuge H, Suzuki J, Isobe M. Telmisartan, a unique ARB, improves left ventricular remodeling of infarcted heart by activating ppar gamma. *Lab Invest* 2011; **91**: 932–944.
- 13 Nagasawa N, Takahashi K, Matsuura N, Takatsu M, Hattori T, Watanabe S, Harada E, Niinuma K, Murohara T, Nagata K. Comparative effects of valsartan in combination with cilnidipine or amlodipine on cardiac remodeling and diastolic dysfunction in Dahl salt-sensitive rats. *Hypertens Res* 2015; **38**: 39–47.
- 14 Ogawa M, Suzuki J, Takayama K, Senbonmatsu T, Hirata Y, Nagai R, Isobe M. Impaired post-infarction cardiac remodeling in chronic kidney disease is due to excessive renin release. *Lab Invest* 2012; **92**: 1766–1776.
- 15 Lewis EJ, Hunsicker LG, Clarke WR, Berl T, Pohl MA, Lewis JB, Ritz E, Atkins RC, Rohde R, Raz I. Renoprotective effect of the angiotensin-receptor antagonist irbesartan in patients with nephropathy due to type 2 diabetes. *N Engl J Med* 2001; **345**: 851–860.
- 16 Jugdutt BI, Menon V. Upregulation of angiotensin II type 2 receptor and limitation of myocardial stunning by angiotensin II type 1 receptor blockers during reperfused myocardial infarction in the rat. *J Cardiovasc Pharmacol Ther* 2003; **8**: 217–226.
- 17 Bongartz LG, Braam B, Verhaar MC, Cramer MJ, Goldschmeding R, Gaillard CA, Doevendans PA, Joles JA. Transient nitric oxide reduction induces permanent cardiac systolic dysfunction and worsens kidney damage in rats with chronic kidney disease. *Am J Physiol Regul Integr Comp Physiol* 2010; **298**: R815–R823.

- 18 Santos LS, Chin EW, Ioshii SO, Tambara Filho R. Surgical reduction of the renal mass in rats: morphologic and functional analysis on the remnant kidney. *Acta Cir Bras* 2006; **21**: 252–257.
- 19 Okada Y, Nakata M, Izumoto H, Takasu M, Tazawa N, Takaoka M, Garipey CE, Yanagisawa M, Matsumura Y. Role of endothelin ETB receptor in partial ablation-induced chronic renal failure in rats. *Eur J Pharmacol* 2004; **494**: 63–71.
- 20 Onai Y, Suzuki J, Maejima Y, Haraguchi G, Muto S, Itai A, Isobe M. Inhibition of NF- $\kappa$ B improves left ventricular remodeling and cardiac dysfunction after myocardial infarction. *Am J Physiol Heart Circ Physiol* 2007; **292**: H530–H538.
- 21 Tsukuda K, Mogi M, Iwanami J, Min LJ, Jing F, Oshima K, Horiuchi M. Irbesartan attenuates ischemic brain damage by inhibition of MCP-1/CCR2 signaling pathway beyond AT(1) receptor blockade. *Biochem Biophys Res Commun* 2011; **409**: 275–279.
- 22 Ariyoshi Y, Mizumoto K. Pharmacological properties and clinical efficacy of the long-acting angiotensin receptor blocker (ARB) irbesartan. *Nihon Yakurigaku Zasshi* 2009; **133**: 275–280.
- 23 Suzuki J, Ogawa M, Futamatsu H, Kosuge H, Sagesaka YM, Isobe M. Tea catechins improve left ventricular dysfunction, suppress myocardial inflammation and fibrosis, and alter cytokine expression in rat autoimmune myocarditis. *Eur J Heart Fail* 2007; **9**: 152–159.
- 24 Smith RS Jr, Agata J, Xia CF, Chao L, Chao J. Human endothelial nitric oxide synthase gene delivery protects against cardiac remodeling and reduces oxidative stress after myocardial infarction. *Life Sci* 2005; **76**: 2457–2471.
- 25 Kameda Y, Hasegawa H, Kubota A, Tadokoro H, Kobayashi Y, Komuro I, Takano H. Effects of pitavastatin on pressure overload-induced heart failure in mice. *Circ J* 2012; **76**: 1159–1168.
- 26 Suzuki J, Ogawa M, Maejima Y, Isobe K, Tanaka H, Sagesaka YM, Isobe M. Tea catechins attenuate chronic ventricular remodeling after myocardial ischemia in rats. *J Mol Cell Cardiol* 2007; **42**: 432–440.
- 27 Tsang SW, Zhang H, Lin C, Xiao H, Wong M, Shang H, Yang ZJ, Lu A, Yung KK, Bian Z. Rhein, a natural anthraquinone derivative, attenuates the activation of pancreatic stellate cells and ameliorates pancreatic fibrosis in mice with experimental chronic pancreatitis. *PLoS ONE* 2013; **8**: e82201.
- 28 Sonomura K, Okigaki M, Kimura T, Matsuoka E, Shiotsu Y, Adachi T, Kado H, Ishida R, Kusaba T, Matsubara H, Mori Y. The kinase Pyk2 is involved in renal fibrosis by means of mechanical stretch-induced growth factor expression in renal tubules. *Kidney Int* 2012; **81**: 449–457.
- 29 Siddesha JM, Valente AJ, Sakamuri SS, Yoshida T, Gardner JD, Somanna N, Takahashi C, Noda M, Chandrasekar B. Angiotensin II stimulates cardiac fibroblast migration via the differential regulation of matrixins and reck. *J Mol Cell Cardiol* 2013; **65**: 9–18.
- 30 Balakumar P, Jagadeesh G. A century old renin-angiotensin system still grows with endless possibilities: At1 receptor signaling cascades in cardiovascular pathophysiology. *Cell Signal* 2014; **26**: 2147–2160.
- 31 Szymanski MK, Buikema JH, van Veldhuisen DJ, Koster J, van der Velden J, Hamdani N, Hillege JL, Schoemaker RG. Increased cardiovascular risk in rats with primary renal dysfunction; mediating role for vascular endothelial function. *Basic Res Cardiol* 2012; **107**: 242.
- 32 Bongartz LG, Braam B, Gaillard CA, Cramer MJ, Goldschmeding R, Verhaar MC, Doevendans PA, Joles JA. Target organ cross talk in cardiorenal syndrome: animal models. *Am J Physiol Renal Physiol* 2012; **303**: F1253–F1263.
- 33 Hoogwerf BJ. Renin-angiotensin system blockade and cardiovascular and renal protection. *Am J Cardiol* 2010; **105**: 30a–35a.
- 34 Chrysant SG. Angiotensin II receptor blockers in the treatment of the cardiovascular disease continuum. *Clin Ther* 2008; **30** (Pt 2): 2181–2190.
- 35 Brunner HR. The new angiotensin II receptor antagonist, irbesartan: pharmacokinetic and pharmacodynamic considerations. *Am J Hypertens* 1997; **10**: 311s–317s.
- 36 Fujino M, Miura S, Kiya Y, Tominaga Y, Matsuo Y, Karnik SS, Saku K. A small difference in the molecular structure of angiotensin II receptor blockers induces at(1) receptor-dependent and -independent beneficial effects. *Hypertens Res* 2010; **33**: 1044–1052.
- 37 Bramlage P, Durand-Zaleski I, Desai N, Pirk O, Hacker C. The value of irbesartan in the management of hypertension. *Expert Opin Pharmacother* 2009; **10**: 1817–1831.
- 38 Croom KF, Curran MP, Goa KL, Perry CM. Irbesartan: a review of its use in hypertension and in the management of diabetic nephropathy. *Drugs* 2004; **64**: 999–1028.
- 39 Kusunoki H, Taniyama Y, Rakugi H, Morishita R. Cardiac and renal protective effects of irbesartan via peroxisome proliferator-activated receptor $\gamma$ -hepatocyte growth factor pathway independent of angiotensin II type 1a receptor blockade in mouse model of salt-sensitive hypertension. *J Am Heart Assoc* 2013; **2**: e000103.
- 40 Vanhoutte D, Schellings M, Pinto Y, Heymans S. Relevance of matrix metalloproteinases and their inhibitors after myocardial infarction: a temporal and spatial window. *Cardiovasc Res* 2006; **69**: 604–613.
- 41 Anzai T. Post-infarction inflammation and left ventricular remodeling: a double-edged sword. *Circ J* 2013; **77**: 580–587.
- 42 Vilahur G, Juan-Babot O, Pena E, Onate B, Casani L, Badimon L. Molecular and cellular mechanisms involved in cardiac remodeling after acute myocardial infarction. *J Mol Cell Cardiol* 2011; **50**: 522–533.
- 43 Bujak M, Frangogiannis NG. The role of TGF- $\beta$  signaling in myocardial infarction and cardiac remodeling. *Cardiovasc Res* 2007; **74**: 184–195.
- 44 Nian M, Lee P, Khaper N, Liu P. Inflammatory cytokines and postmyocardial infarction remodeling. *Circ Res* 2004; **94**: 1543–1553.
- 45 Cao W, Zhou QG, Nie J, Wang GB, Liu Y, Zhou ZM, Hou FF. Albumin overload activates intrarenal renin-angiotensin system through protein kinase C and NADPH oxidase-dependent pathway. *J Hypertens* 2011; **29**: 1411–1421.
- 46 Rubattu S, Mennuni S, Testa M, Mennuni M, Pierelli G, Pagliaro B, Gabriele E, Coluccia R, Autore C, Volpe M. Pathogenesis of chronic cardiorenal syndrome: is there a role for oxidative stress? *Int J Mol Sci* 2013; **14**: 23011–23032.
- 47 Chen J, Mehta JL. Angiotensin II-mediated oxidative stress and procollagen-1 expression in cardiac fibroblasts: blockade by pravastatin and pioglitazone. *Am J Physiol Heart Circ Physiol* 2006; **291**: H1738–H1745.
- 48 Zhao QD, Viswanadhapalli S, Williams P, Shi Q, Tan C, Yi X, Bhandari B, Abboud HE. NADPH oxidase 4 induces cardiac fibrosis and hypertrophy through activating Akt/mTOR and NF $\kappa$ B signaling pathways. *Circulation* 2015; **131**: 643–655.
- 49 Cho E, Kim M, Ko YS, Lee HY, Song M, Kim MG, Kim HK, Cho WY, Jo SK. Role of inflammation in the pathogenesis of cardiorenal syndrome in a rat myocardial infarction model. *Nephrol Dial Transplant* 2013; **28**: 2766–2778.
- 50 Dong Z, Wu P, Li Y, Shen Y, Xin P, Li S, Wang Z, Dai X, Zhu W, Wei M. Myocardial infarction worsens glomerular injury and microalbuminuria in rats with pre-existing renal impairment accompanied by the activation of ER stress and inflammation. *Mol Biol Rep* 2014; **41**: 7911–7921.
- 51 Shlipak MG. Pharmacotherapy for heart failure in patients with renal insufficiency. *Ann Intern Med* 2003; **138**: 917–924.
- 52 Nishikimi T, Inaba-Iemura C, Ishimura K, Tadokoro K, Koshikawa S, Ishikawa K, Akimoto K, Hattori Y, Kasai K, Minamino N, Maeda N, Matsuoka H. Natriuretic peptide/natriuretic peptide receptor-a (NPR-a) system has inhibitory effects in renal fibrosis in mice. *Regul Pept* 2009; **154**: 44–53.